Xue et al. Nanoscale Research Letters (2018) 13:290
https://doi.org/10.1186/s11671-018-2712-1

Nanoscale Research Letters

NANO REVIEW

Open Access

An Overview of the Ultrawide Bandgap Ga_2O_3 Semiconductor-Based Schottky Barrier Diode for Power Electronics Application

Xue HuiWen[1,2], He QiMing[2], Jian GuangZhong[2], Long ShiBing[3*], Pang Tao[1*] and Liu Ming[2,3]

Abstract

Gallium oxide (Ga_2O_3) is a new semiconductor material which has the advantage of ultrawide bandgap, high breakdown electric field, and large Baliga's figure of merit (BFOM), so it is a promising candidate for the next-generation high-power devices including Schottky barrier diode (SBD). In this paper, the basic physical properties of Ga_2O_3 semiconductor have been analyzed. And the recent investigations on the Ga_2O_3-based SBD have been reviewed. Meanwhile, various methods for improving the performances including breakdown voltage and on-resistance have been summarized and compared. Finally, the prospect of Ga_2O_3-based SBD for power electronics application has been analyzed.

Keywords: Gallium oxide (Ga_2O_3), Ultrawide bandgap semiconductor, Power device, Schottky barrier diode (SBD), Breakdown electric field, Baliga's figure of merit, On-resistance

Background

With the fast development of electrical power, industrial control, automotive electronics, and consumer electronics industries, there is a huge demand for high-performance power semiconductor devices. Wide and ultrawide bandgap semiconductor materials can satisfy this demand [1, 2]. Among the five structures of Ga_2O_3 single crystal, monoclinic β-Ga_2O_3 is the most stable, and it has an ultrawide bandgap (E_g~ 4.8 eV) and very high breakdown electric field (E_{br}~ 8 MV cm^{-1}), compared to the traditional Si and later developed SiC and GaN material. In consequence, β-Ga_2O_3 shows a much large Baliga's figure of merit (BFOM = $\varepsilon\mu E_b^3$; ε is the relative dielectric constant, and μ is the electron mobility). BFOM is an important criterion to assess the appropriateness of a material for power device application [3–11]. Table 1 compares the basic physical properties of Si, wide bandgap (GaN, SiC), and ultrawide bandgap (β-Ga_2O_3) semiconductor material. Furthermore, for the growth of single-crystal β-Ga_2O_3 substrate, there are easy, low-cost, and mass-producible melt-growth methods at atmospheric pressure, such as floating zone (FZ) [12, 13] and the edge-defined film-fed growth (EFG) [14–17]. This is another superiority of Ga_2O_3 in the aspect of high-quality single-crystal growth, compared with SiC and GaN. Therefore, β-Ga_2O_3 is a promising candidate for next-generation high-power semiconductor devices such as Schottky barrier diode (SBD) [18–24] and metal-oxide-semiconductor field-effect transistor (MOSFET) [25–29]. It is worth noting that a lot of studies on the Ga_2O_3 material growth and power device fabrication and characterization have been carried out in the last several years, so in this paper, we reviewed the material properties of the ultrawide bandgap Ga_2O_3 semiconductor and the investigations of the Ga_2O_3-based SBD for power electronics application. In SBD, the most important performance parameters are breakdown voltage (V_{br}) and on-resistance (R_{on}), so through summarizing and comparing the various methods for improving the V_{br} and R_{on} performances, we wish our reviewing work is

* Correspondence: shibinglong@ustc.edu.cn; longshibing@ime.ac.cn; 12773@sicau.edu.cn
[3]School of Microelectronics, University of Science and Technology of China, Hefei 230026, China
[1]College of Mechanical and Electrical Engineering, Sichuan Agricultural University, Yaan 625014, China
Full list of author information is available at the end of the article

Springer Open

© The Author(s). 2018 **Open Access** This article is distributed under the terms of the Creative Commons Attribution 4.0 International License (http://creativecommons.org/licenses/by/4.0/), which permits unrestricted use, distribution, and reproduction in any medium, provided you give appropriate credit to the original author(s) and the source, provide a link to the Creative Commons license, and indicate if changes were made.

Table 1 Comparison of the physical properties of Si, GaN, SiC, and β-Ga_2O_3 semiconductor [5]

Semiconductor material	Si	GaN	4H-SiC	β-Ga_2O_3
Bandgap E_g (eV)	1.1	3.4	3.3	4.7–4.9
Electron mobility μ (cm^2 V^{-1} s^{-1})	1400	1200	1000	300
Breakdown electric field E_{br} (MV/cm)	0.3	3.3	2.5	8
Baliga's FOM ($\varepsilon\mu E_b^3$)	1	870	340	3444
Thermal conductivity λ (W cm^{-1} K^{-1})	1.5	2.1	2.7	0.11

beneficial for the development of Ga_2O_3-based power devices.

Physical Properties of Gallium Oxide Semiconductor

Gallium oxide (Ga_2O_3) is a new oxide semiconductor material, but it has a long research history. The investigation on the phase equilibria in the Al_2O_3-Ga_2O_3-H_2O system can be traced back to 1952, and R. Roy et al. determined the existence of polymorphs of Ga_2O_3 and their stability relations [30]. In 1965, H. H. Tippins et al. studied the optical absorption and photoconductivity in the band edge of β-Ga_2O_3 and confirmed its bandgap with a value of 4.7 eV [6]. In 1990s, a number of methods on the melting growth of Ga_2O_3 bulk single-crystal and epitaxial growth of Ga_2O_3 film had been developed. In recent 5 years, owing to its special properties and the successful growth of high-quality and large-size single-crystal substrate, Ga_2O_3 material has attracted a lot of research interest.

Till now, people have found five crystalline phases of Ga_2O_3, i.e., α, β, γ, δ, and ε phases. The transformation relationships among these five phases are shown in Fig. 1 [30]. The monoclinic phase β-Ga_2O_3 has the best thermal stability, while the other four phases are metastable and are apt to transform to β-Ga_2O_3 at high temperatures. Therefore, at present, most studies focus on β-Ga_2O_3. Some recent investigations also found that other phases presented some special material properties which β phase did not have. For example, α-Ga_2O_3 has a corundum crystal structure similar to that of sapphire (Al_2O_3), so it is comparatively easy to epitaxially grow high-quality α-Ga_2O_3 single-crystal film on the currently existing Al_2O_3 single-crystal substrate. Hexagonal phase ε-Ga_2O_3 is the second stable phase and presents strong spontaneous polarization effect which is beneficial to form high-density 2D electron gas in the heterojunction interface [31], similar to the condition in AlGaN/GaN junction. In recent years, due to the successful growth of large-size β-Ga_2O_3 single-crystal substrate and its best stability, up to now, the studies on β-Ga_2O_3 are far more than those on the other four phases. So, in this paper, we mainly review the research works on β-Ga_2O_3.

β-Ga_2O_3 belongs to monoclinic system and is thermally stable. Its lattice constants are a = 1.22 nm, b = 0.30 nm, and c = 0.58 nm, as shown in Fig. 2. The crystalline structure of β-Ga_2O_3 determines that it has a certain conductivity, but which is limited by its ultrawide bandgap (4.7–4.9 eV), the widest one of all the known transparent semiconductor materials. Only if some defect energy levels exist in the bandgap and free electrons generate, the material has comparatively strong conductivity. For most wide bandgap semiconductors, conductivity is formed just because of the existence of defect levels in bandgap, such as ZnO semiconductor [32]. The intrinsic electrical conduction of β-Ga_2O_3 originates from the free electrons led by the point defects formed in the bulk of crystal.

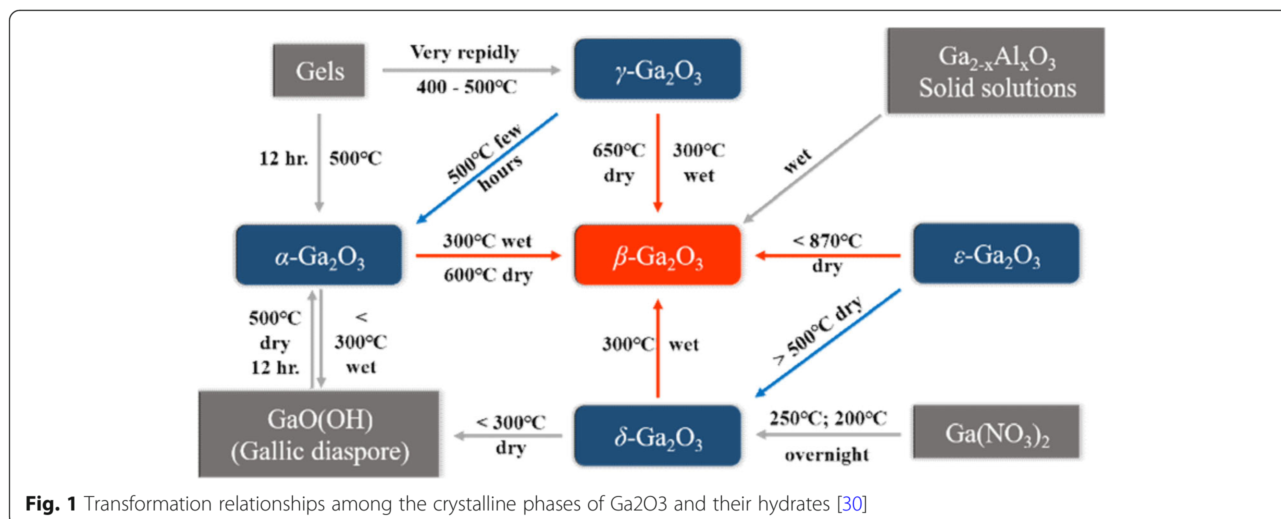

Fig. 1 Transformation relationships among the crystalline phases of Ga2O3 and their hydrates [30]

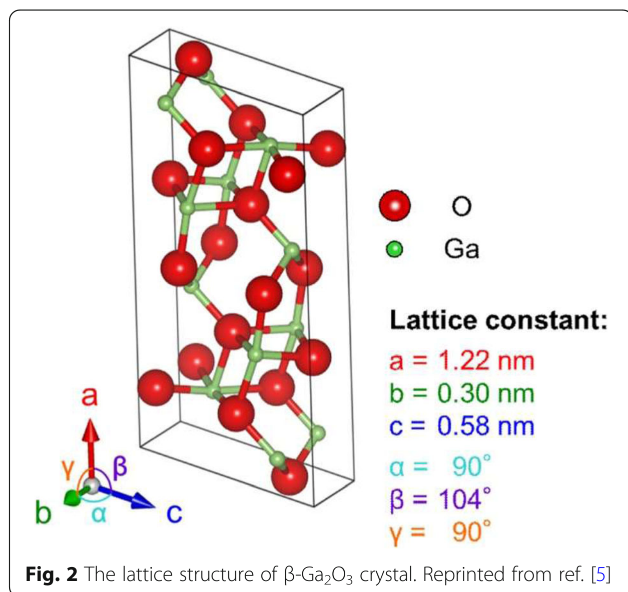

Fig. 2 The lattice structure of β-Ga_2O_3 crystal. Reprinted from ref. [5]

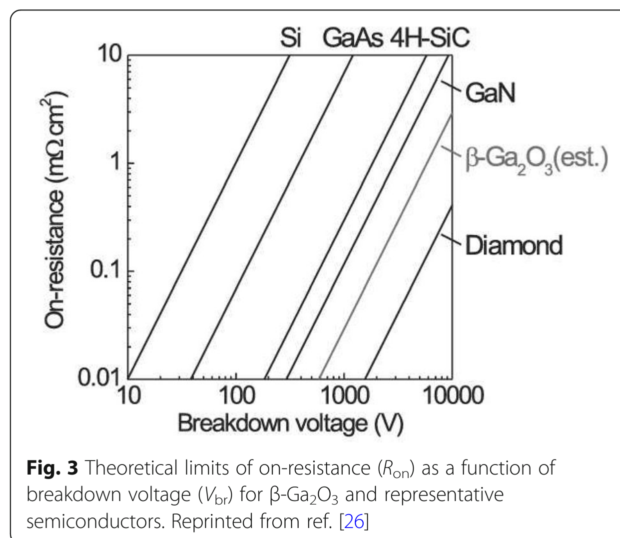

Fig. 3 Theoretical limits of on-resistance (R_{on}) as a function of breakdown voltage (V_{br}) for β-Ga_2O_3 and representative semiconductors. Reprinted from ref. [26]

Most studies have demonstrated that the oxygen vacancies are the key defects for the electrical conduction [33–35].

It is interesting that due to the existence of the plenty of oxygen vacancies in polycrystalline β-Ga_2O_3, it is easy to absorb some kind of gas to make the resistivity change, so there have been many reports about using β-Ga_2O_3 to fabricate gas sensors for the detection of H_2, CH_4, CO, and O_2 [36–39]. In addition, because the lattice constant of β-Ga_2O_3 in [100] direction is much larger than those in [001] and [010] directions, it is easy to peel off ultrathin film along [100] direction for device fabrication [27, 40–43]. At the same time, owing to this crystal structure characteristic, in the fabrication of β-Ga_2O_3 wafers, cutting the bulk along [100] direction can acquire flat surface with very low roughness.

Compared to SiC and GaN, β-Ga_2O_3 possesses particular electrical characteristics, among which the ultrawide bandgap (4.7–4.9 eV) is the most prominent. This makes it have a very high critical breakdown electrical field (E_{br}≈8 MV/cm), about twice those of SiC and GaN. The breakdown electrical field of material is a very important parameter for unipolar power devices. If a material has higher E_{br}, in the material of unit thickness, higher electrical field can be maintained, which is advantageous for the reduction of device size and enhancement of the integration level of power modules. Figure 3 shows the fundamental limits of on-resistance (R_{on}) as a function of breakdown voltage (V_{br}) for several important semiconductors including Si, GaAs, SiC, GaN, Ga_2O_3, and diamond [5]. From this figure, we can find that the conduction loss of Ga_2O_3 devices is one order of magnitude lower than those of SiC and GaN devices at the same V_{br}. Thus, Ga_2O_3 shows its great potential in unipolar devices. As the saturation electron mobility of β-Ga_2O_3 is comparatively low (~ 200 cm^2 V^{-1} s^{-1}), β-Ga_2O_3 is not suitable for high-frequency devices compared to GaN. However, its wide bandgap can compensate for this disadvantage since thinner drift layer has smaller depletion width; thus, the parasitic capacitance can be decreased to meet the requirements of high-frequency applications. Besides, the bandgap of about 4.8 eV makes Ga_2O_3 possess special absorption wave band (250–280 nm) which is just located in the range of solar blind ultraviolet (UV) ray, so Ga_2O_3 is a natural good material for fabricating UV detectors [44–47].

In recent years, the n-type doping of β-Ga_2O_3 has been basically realized. Si and Sn elements, as its donor impurities with shallow energy level, have low-activation energy. Doping concentration can be well modulated to be in the range of 10^{15}–10^{19} cm^{-3} [47], with the highest value of 10^{20} cm^{-3} reached. At the same time, with the change of doping concentration, the optical and electrical properties will also change. For example, the resistivity of n-type β-Ga_2O_3 changes in the range of 10^{-3} – 10^{12} Ω cm with the changing doping concentration [48, 49]. The bandgap also changes with different doping concentration, so the light absorption characteristics of Ga_2O_3 are influenced [50].

From the development of Ga_2O_3, this material still has some disadvantages as follows. (1) P-type doping is a big challenge of Ga_2O_3 material. Because the acceptor levels are far from the valence band of β-Ga_2O_3, the activation energy of acceptor impurities is very high. Meanwhile, the n-type background impurities in Ga_2O_3 crystal will also produce self-compensation effect on acceptor impurities, resulting to the self-insulating of the material. Therefore, there still has been no effective p-type doing.

(2) The thermal conductivity of Ga_2O_3 is too low. Experimental and theoretical investigations have proved that the thermal conductivity of β-Ga_2O_3 is just only 0.1–0.3 W cm^{-1} K^{-1} [51–53]. This is adverse to the power device used in high-voltage and high-current circumstance. Excessive heat accumulation will seriously affect the performance and reliability of the device. (3) Carrier mobility is low. The theoretical mobility of Ga_2O_3 is limited to about 200 cm^2/V s due to the influence of scattering [54]. Low mobility has a negative impact on the frequency and current characteristics.

The Basic Concept of Schottky Barrier Diode

Schottky contact, ohmic contact, and electrical field distribution are the key factors in SBD to attain high performances including on-resistance (R_{on}) and breakdown voltage (V_{br}), so various methods for improving them are especially important.

According to the concept of Schottky barrier, the barrier height is related to the work function of Schottky metal and the electron affinity of semiconductor. The work function of different metals changes periodically, and metal needs to have larger work function than semiconductor in order to form Schottky barrier. Nickel (Ni) and platinum (Pt) are the common Schottky metals for β-Ga_2O_3, and their barrier heights are derived with diverse methods [55–77]. The depletion region under the surface of semiconductor needs necessary thickness to prevent carrier tunneling, and this requires the limited doping concentration of semiconductor. Common values of doping concentration are 10^{16}–10^{17} cm^{-3} in the β-Ga_2O_3 substrate or epitaxy layer [56–62]. The barrier height is actually affected by the interface states and deviates from a simple relationship with work function. The surface pre-treatment aims to reduce the interface states, including the near-surface oxygen vacancies and dangling bonds [78].

The ohmic contact is the basic link between metal and semiconductor. A low-specific resistance of ohmic contact is helpful for the devices to decrease contact resistance (R_s) and on-resistance (R_{on}). The traditional methods to achieve low-contact resistance are choosing low-work function metal and heavy doping. In fact, the work function of contact metal is always uninfluential for the formation of ohmic contact due to the pinning of interface states. The heavy doping of semiconductor becomes the primary technique for the ohmic contact. The main targets are improving the concentration of carriers and lowering the interface barrier. The RTA (rapid thermal annealing) improves the interfacial characteristics and redounds to reducing the contact resistance. Y. Yao et al. tested nine metals as ohmic contact metals to the β-Ga_2O_3 and found that titanium (Ti) and indium (In) show good ohmic behavior under specific conditions [79]. After annealing in high temperatures, only titanium can maintain the continuous morphology. Similar to this, most studies applied titanium as the ohmic contact metal with β-Ga_2O_3 and obtained favorable device performances [60–70].

The breakdown behavior is related to the distribution of electric field inside the devices, and cylindrical junction and spherical junction have larger electric field than parallel-plane junction in the same condition [1]. Therefore, some edge termination protection methods are needed such as field plate to enhance the breakdown voltage [19, 23, 68]. The interface states referred as interface charges normally impact the electric field close to the semiconductor surface and cause the premature breakdown. The leakage current is the indicator of breakdown behavior and is commonly affected by the internal defects of semiconductor, including dislocations. Both situations cause the instability of devices and may decrease the breakdown voltage which should be avoided. The common practice for reducing the impact of interface states is surface passivation, and high-quality substrate is also required for increasing the breakdown voltage.

Schottky Barrier Diode Based on β-Ga_2O_3

The difficulties in the growth of high-quality and low-cost single-crystal substrates have affected the commercialization of SiC and GaN devices. While Ga_2O_3 single-crystal substrates can be grown by low-cost melting method, the power devices based on Ga_2O_3 single crystal have attracted much attention in recent years. At present, the n-type doping technology of Ga_2O_3 is quite mature, but the lack of p-type doping makes Ga_2O_3 unable to be applied into bipolar devices. The ultra large bandgap makes it a big advantage in the application of unipolar devices. Therefore, the development of the Ga_2O_3 power devices is dominated by two kinds of unipolar devices, i.e., the Schottky barrier diode (SBD) and metal-oxide-semiconductor field-effect transistor (MOSFET) [23, 55, 56].

With the development of the wide bandgap (WBG) semiconductor material technology, the SBD device based on WBG semiconductor begins to replace p-n junction diode to apply into power electronic system because no minority carrier storage effect exists in SBD and its switching loss is quite low. In theory, compared to SiC and GaN SBD, Ga_2O_3 SBD can achieve the same breakdown voltage with much thinner drift layer. At the same time, thinner drift layer makes lower parasitic capacitance, shortening the reverse recovery time of the device. The main development progress of Ga_2O_3 SBD is shown in Fig. 4. With the development of the epitaxy technology, the SBD structure has developed from the initial substrate-based simple structure to the substrate and epitaxial film-based complex structure. Subsequently,

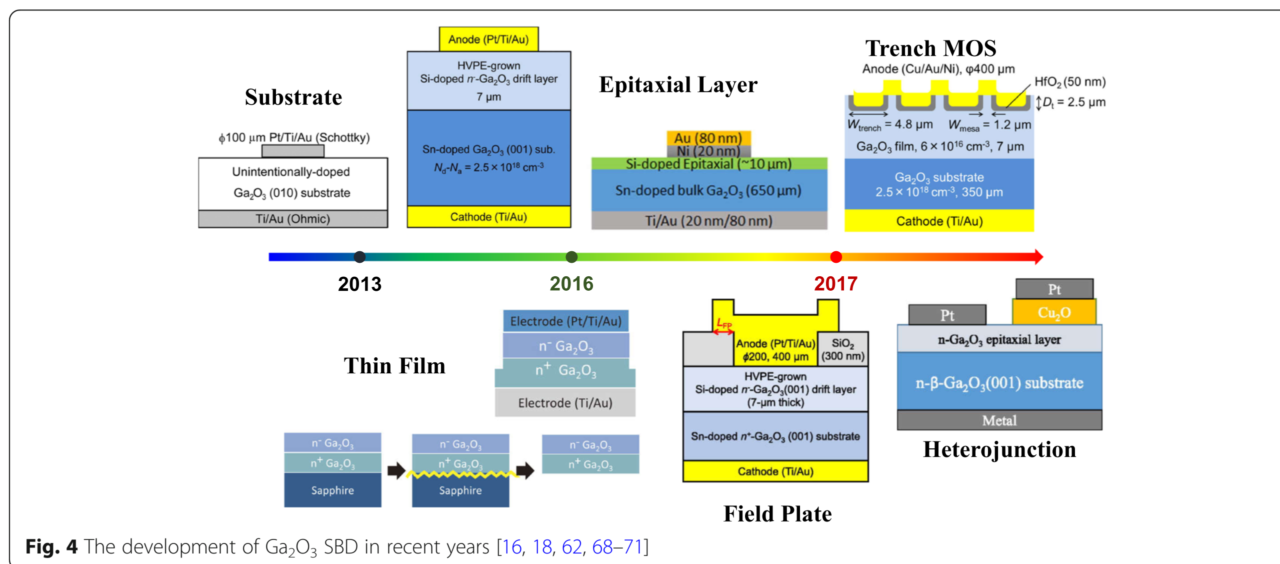

Fig. 4 The development of Ga_2O_3 SBD in recent years [16, 18, 62, 68–71]

through the gradual exploration on the device fabrication processes, advanced terminal structures including filed plate and trench have appeared, further enhancing the device performances. Ga_2O_3 SBD starts to present its potential in power electronics applications.

As a new wide bandgap semiconductor material, people confronted a lot of basic problems in the initial development stage of Ga_2O_3, so the development progress of Ga_2O_3 SBD reflexes the evolution of power SBD very well. The most important part in SBD is the Schottky junction, so in the early research works on Ga_2O_3 SBD, there are a substantial numbers of ones focusing on the study on the Schottky junction, mainly including the contact between Ga_2O_3 and different Schottky electrodes (Ni、Cu、Au、Pt、TiN) [57–59], the electron transport mechanism of the Schottky junction, the issues of interface states, barrier inhomogeneity and image force existing in the Schottky contact, and the methods of how to acquire perfect ohmic contact in the cathode interface [60, 61].

With the gradual perspicuousness of the physical properties and the increasingly improvement of the fabrication processes, the device performances are progressively enhanced. The following are some typical works in the development of Ga_2O_3 SBD.

In 2013, K. Sasaki et al. in Tamura Corporation fabricated SBD based on high-quality (010) β–Ga_2O_3 single-crystal substrate grown by floating zone method [62]. They investigated the impact of the different doping concentration in the substrate on the device performance and found that higher doping concentration induced lower on-resistance but lower reverse breakdown voltage and larger reverse leakage current. Figure 5

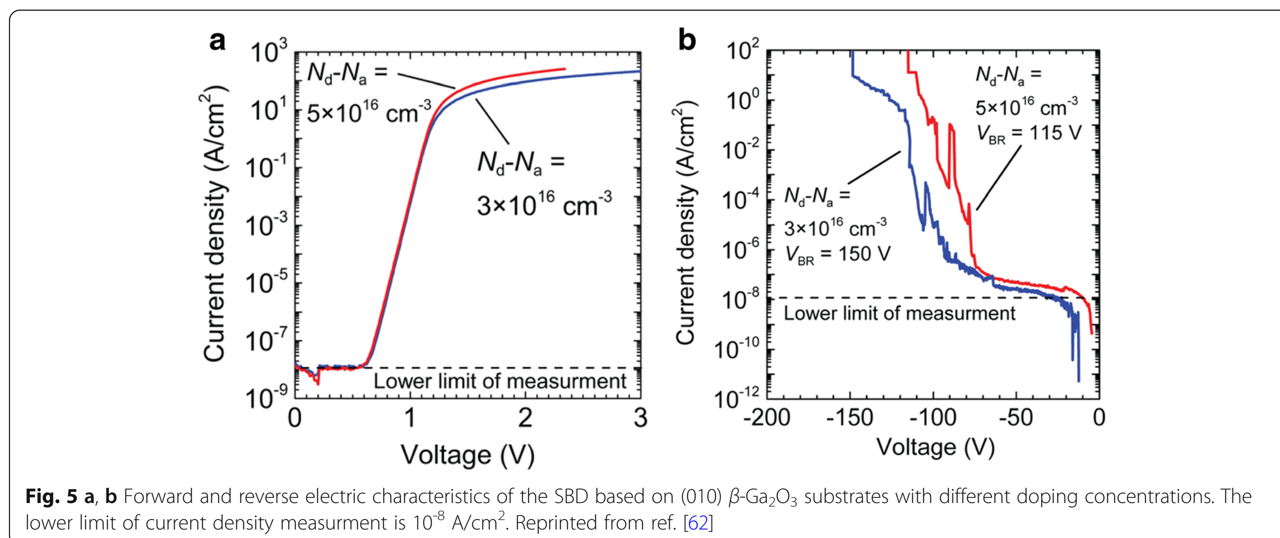

Fig. 5 **a**, **b** Forward and reverse electric characteristics of the SBD based on (010) β-Ga_2O_3 substrates with different doping concentrations. The lower limit of current density measurment is 10^{-8} A/cm^2. Reprinted from ref. [62]

shows the reverse breakdown characteristics of the two SBDs fabricated with (010) β–Ga_2O_3 substrates with different doping concentrations. The breakdown voltage reaches 150 V. The ideality factor of both devices is close to 1. And the Schottky barrier height of the Pt/β–Ga_2O_3 interface was estimated to be 1.3–1.5 eV.

Researchers from Institute of Microelectronics of Chinese Academy of Sciences (IMECAS) and Shandong University have collaborated to investigate the SBD based on (100)-oriented β–Ga_2O_3 bulk substrate. In 2017, they reported a Pt/β–Ga_2O_3 SBD and its temperature-dependent electrical characteristics. X-ray diffraction (XRD) and high-resolution transmission electron microscopy (HRTEM) analysis showed that the β–Ga_2O_3 bulk single crystal grown by edge-defined film-fed growth (EFG) technique presented good (100) orientation and good crystal quality (Figs. 6a, b). Through I–V measurements and thermionic emission modeling, the fabricated Pt/β–Ga_2O_3 SBD device exhibited good performances, including rectification ratio of 10^{10}, ideality factor (n) of 1.1, Schottky barrier height (Φ_B) of 1.39 eV, threshold voltage (V_{bi}) of 1.07 V, on-resistance (R_{on}) of 12.5 mΩ cm^2, forward current density at 2 V ($J_{@2V}$) of 56 A/cm^2, and effective donor concentration ($N_d - N_a$) of 2.3×10^{14} cm^{-3} (Figs. 6c, d). Good temperature-dependent performance was also found in the device (Figs. 6e, f). With the increase of temperature, R_{on}

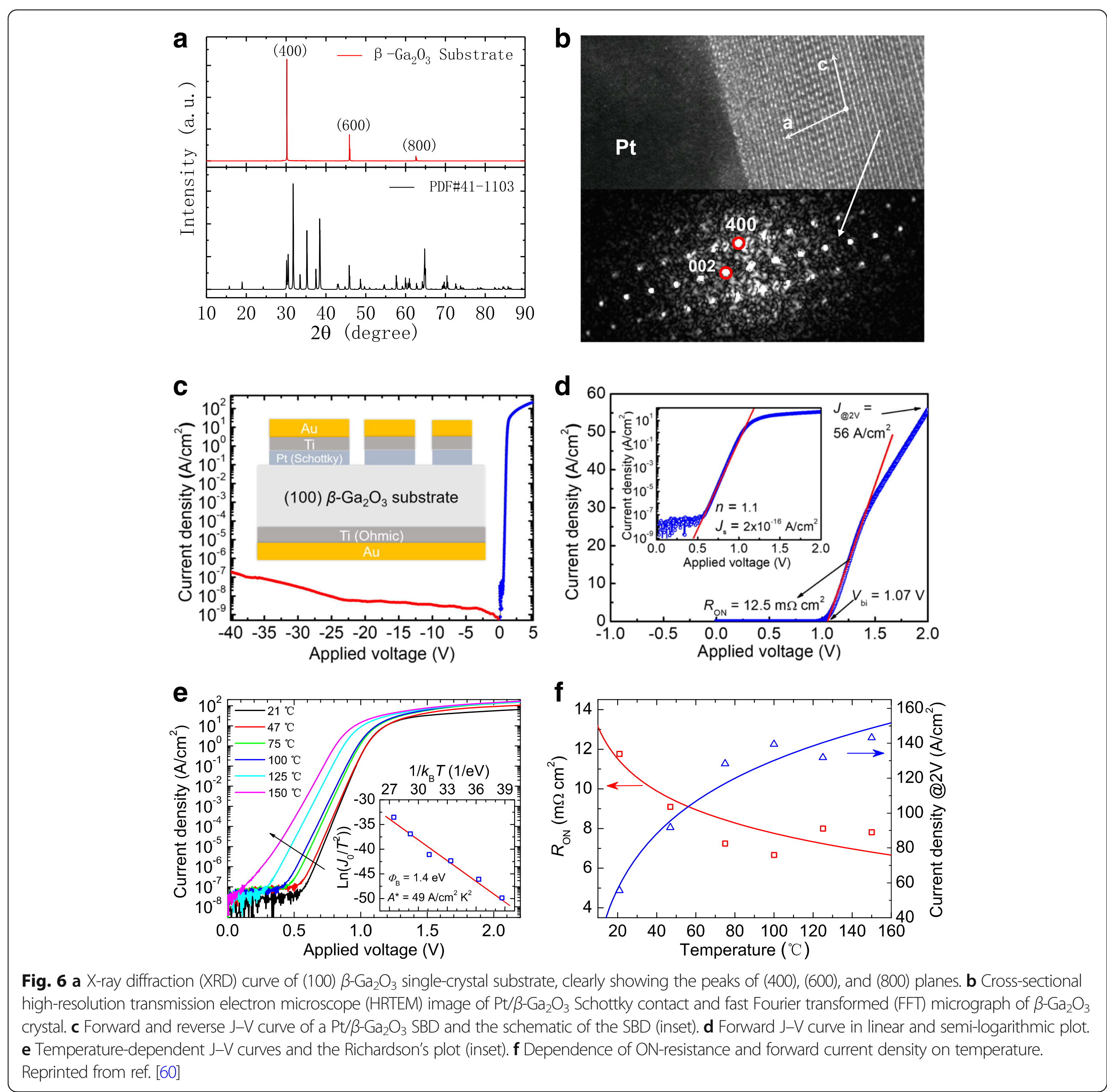

Fig. 6 **a** X-ray diffraction (XRD) curve of (100) β-Ga_2O_3 single-crystal substrate, clearly showing the peaks of (400), (600), and (800) planes. **b** Cross-sectional high-resolution transmission electron microscope (HRTEM) image of Pt/β-Ga_2O_3 Schottky contact and fast Fourier transformed (FFT) micrograph of β-Ga_2O_3 crystal. **c** Forward and reverse J–V curve of a Pt/β-Ga_2O_3 SBD and the schematic of the SBD (inset). **d** Forward J–V curve in linear and semi-logarithmic plot. **e** Temperature-dependent J–V curves and the Richardson's plot (inset). **f** Dependence of ON-resistance and forward current density on temperature. Reprinted from ref. [60]

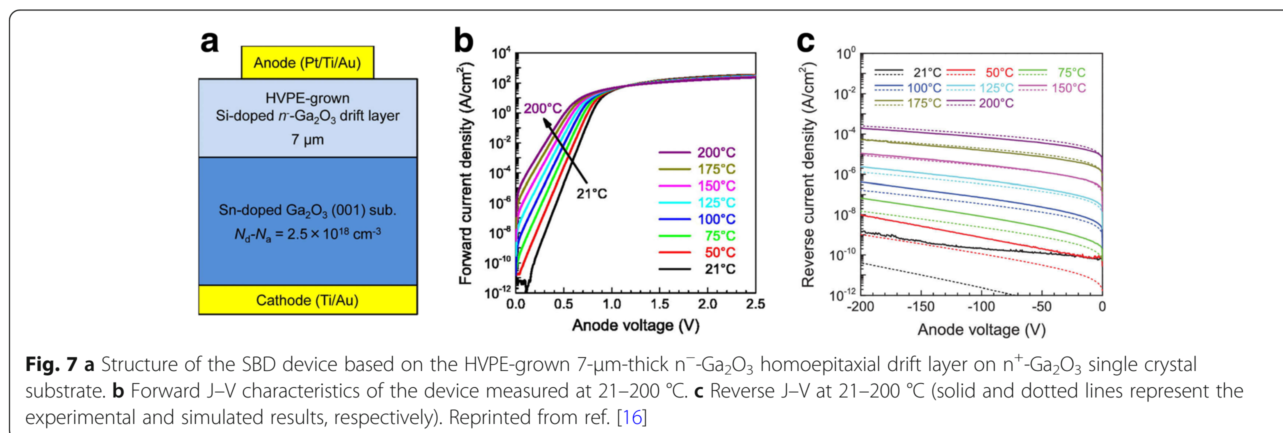

Fig. 7 **a** Structure of the SBD device based on the HVPE-grown 7-μm-thick n^{-}-Ga_2O_3 homoepitaxial drift layer on n^{+}-Ga_2O_3 single crystal substrate. **b** Forward J–V characteristics of the device measured at 21–200 °C. **c** Reverse J–V at 21–200 °C (solid and dotted lines represent the experimental and simulated results, respectively). Reprinted from ref. [16]

and $J_{@2V}$ became better, demonstrating that the device could work well at high temperature. In their following work, they further deeply investigated the temperature dependence of ideality factor and Schottky barrier height and found that this kind of temperature characteristics can be explained by the Gaussian distribution of barrier height inhomogeneity [61]. In 2018, they further optimized crystal growth parameters and improved the Sn doping concentration ($N_d - N_a = 2.3 \times 10^{14}$ cm^{-3}). The new Pt/β–Ga_2O_3 SBD device shows markedly improved performance, including forward current density ($J_{@2V}$ = 421 A/cm^2), ON-state resistance ($R_{on} = 2.9$ mΩ cm^2), a short reverse recovery time (20 ns), and a reverse breakdown voltage higher than 200 V [63]. Their work indicates that EFG grown β–Ga_2O_3 single crystal is a promising for power device application.

Q. Feng et al. from Xidian University have studied the pulsed laser deposition (PLD) preparation processes and the basic physical properties of the Al-doped β–Ga_2O_3 film [64–66]. Doping Al is able to tune the bandgap of β–Ga_2O_3 by incorporating different Al atom ratios. Based on this kind Al-doped film, Ni/β-$(AlGa)_2O_3$ SBD device was fabricated and characterized. The Schottky barrier height is 1.33 eV. The current on-off ratio and on-resistance reach 10^{11} and 2.1 mΩ cm^2, respectively [65]. They also studied the influence of the temperature on the ideality factor and Schottky barrier height and also got the conclusion that these temperature dependence characteristics of n and Φ_B were attributed to the Schottky barrier inhomogeneities by assuming the existence of a Gaussian distribution of the barrier height [66].

With the development of the film epitaxy technology, halide vapor-phase epitaxy (HVPE) was utilized to grow Ga_2O_3 film. Owing to the advantages of rapid speed of the epitaxy and high quality of the film, HVPE-grown Ga_2O_3 is very suitable for fabricating the drift layer of the high-voltage SBD. In 2015, M. Higashiwaki et al. in the National Institute of Information and Communications Technology (NICT) grew 7-μm-thick lightly doped ($\sim 1 \times 10^{16}$ cm^{-3}) epitaxial layer on the heavily doped ($N_d - N_a = 2.5 \times 10^{18}$ cm^{-3}) (001) β-Ga_2O_3 substrate through HVPE method and further fabricated SBD device. The C–V and I–V characteristics of the device at different temperatures were investigated. The change trend of the Schottky barrier height, threshold voltage, C–V and I–V curves with temperature was pointed out. Figure 7 shows the device structure and the forward and reverse J–V–T curves [16]. It was found that at 21–200 °C, the barrier height kept nearly constant. The forward and reverse current agreed well with the thermionic emission (TE) and thermionic field emission (TFE) model, respectively. Their results demonstrated the potential of the application of the Ga_2O_3 SBD in next-generation power devices.

In 2016, M. Oda et al. in FLOSFIA Inc. published a work about α-Ga_2O_3 SBD [18]. Through a mist chemical vapor deposition (CVD) technique, i.e., MIST EPITAXY®, they successively grew heavily (3–4 μm thick) and lightly

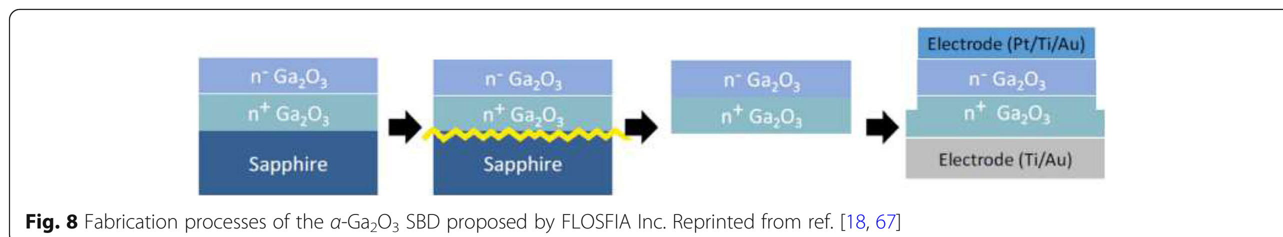

Fig. 8 Fabrication processes of the α-Ga_2O_3 SBD proposed by FLOSFIA Inc. Reprinted from ref. [18, 67]

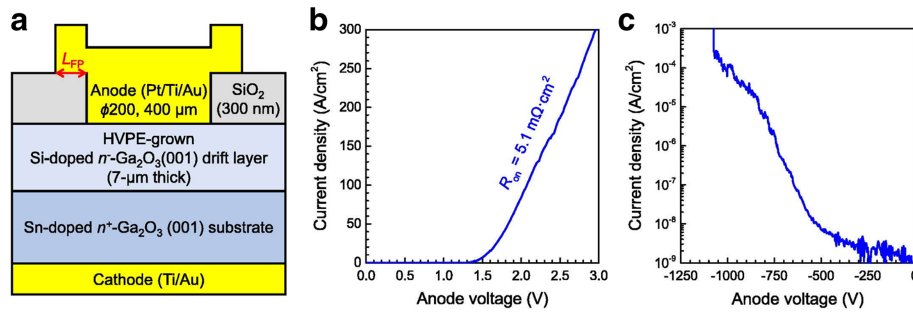

Fig. 9 a Structure of the SBD with field plate. **b**, **c** Forward and reverse electrical characteristics (V_{br} = 1076 V). Reprinted from ref. [68]

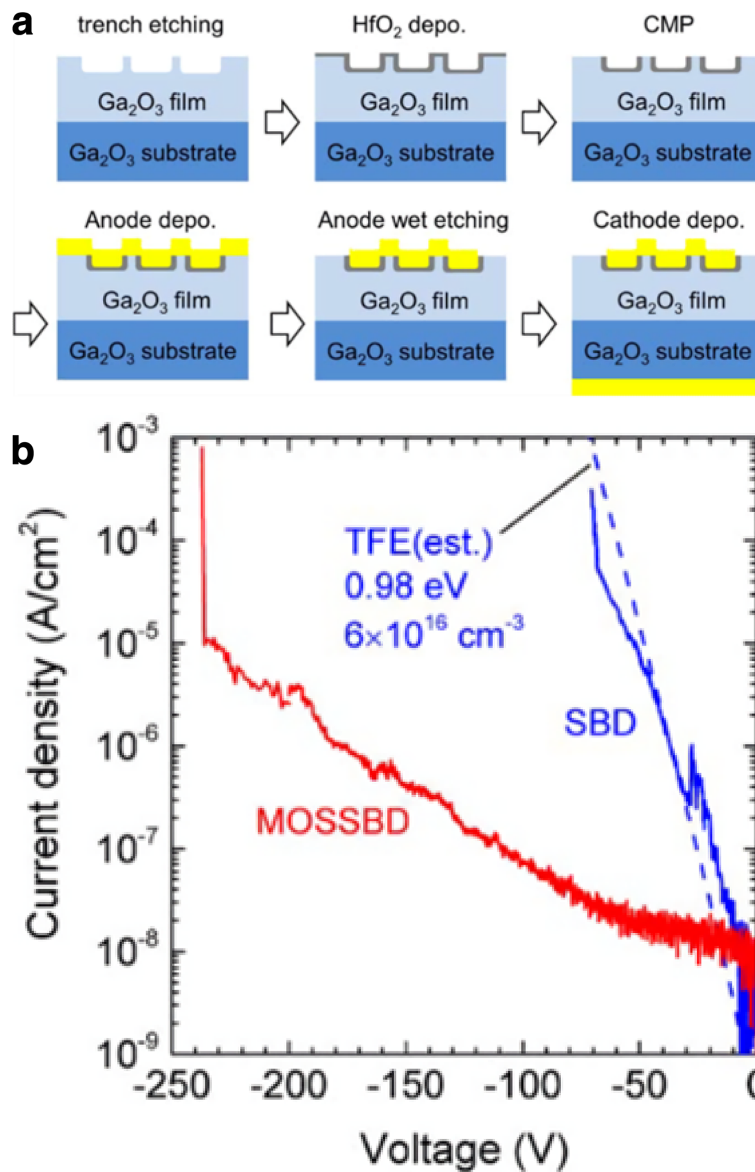

Fig. 10 a Fabrication processes of the MOS-type Ga_2O_3 SBD with trench termination structure. **b** Comparison of the reverse characteristics of the Ga_2O_3 SBDs with and without trenches. Reprinted from ref. [70]

doped α-Ga_2O_3 films on sapphire (Al_2O_3) substrates. After lifting off the α-Ga_2O_3 layers from the substrates, cathode and anode were deposited on the bottom and top surface of the n^--Ga_2O_3/n^+-Ga_2O_3 layers, respectively (Fig. 8). The device with a 2580-nm-thick n^--Ga_2O_3 layer showed a high breakdown voltage of 855 V and an on-resistance of 0.4 mΩ cm^2. While the device with a thinner (430 nm) n^--Ga_2O_3 layer SBDs exhibited a very low on-resistance of 0.1 mΩ cm^2 and a breakdown voltage of 531 V. In 2018, they further reported this kind of device conducted with a TO220 package [67]. A junction capacitance of 130 pF was got, so the device showed a better reverse recovery characteristic compared with SiC SBD and Si SBD. At the same time, after package, the device exhibited a thermal resistance of 13.9 °C/W, comparable to that of the SiC SBD with the same package (12.5 °C/W), demonstrating that adopting thin drift layer can effectively compensate the disadvantage of the bad thermal conductivity of Ga_2O_3 material. In this report the authors also pointed out that α-$(Rh,Ga)_2O_3$ can act as an effective p-type channel layer of α-Ga_2O_3 devices.

In 2017, K. Konishi et al. in NICT reported a Pt/HVPE-n^--Ga_2O_3/(001)n^+-Ga_2O_3 SBD device with a breakdown voltage of 1076 V and an on-resistance of 5.1 mΩ cm^2 (Fig. 9) [68]. Field plate (FP) engineering, a kind of edge termination technology, was first used into Ga_2O_3 SBD. By adding an anode connected SiO_2 FP, the maximum electric field in the entire device structure was kept below the critical field, especially the electric field around the anode can be obviously decreased. Employing this method, both high breakdown voltage and low on-resistance can be achieved. In the same year, a higher breakdown voltage (1600 V) was reported by J. Yang, et al. from the University of Florida in their SBD device with a Ni/MOCVD-n^--Ga_2O_3/(− 201) n^+-Ga_2O_3 structure [69], but the on-resistance is very large (25 mΩ cm^2). No edge termination was used. Their investigation showed that the size of the Schottky electrode had an influence on the breakdown voltage and on-resistance because larger electrode would have more defects and lead to easier breakdown.

In 2017, K. Sasaki et al. from Novel Crystal Technology Inc. first fabricated β-Ga_2O_3 SBD with trench termination structure (Fig. 10) [70]. By adopting this kind of structure, the electric field in the Schottky junction can be effectively decreased; thus, the leakage current can be greatly reduced while the forward properties are well maintained. The on-resistance of the device was 2.9 mΩ cm^2, and the breakdown voltage reached about 240 V. At the same time, the threshold voltage was remarkably

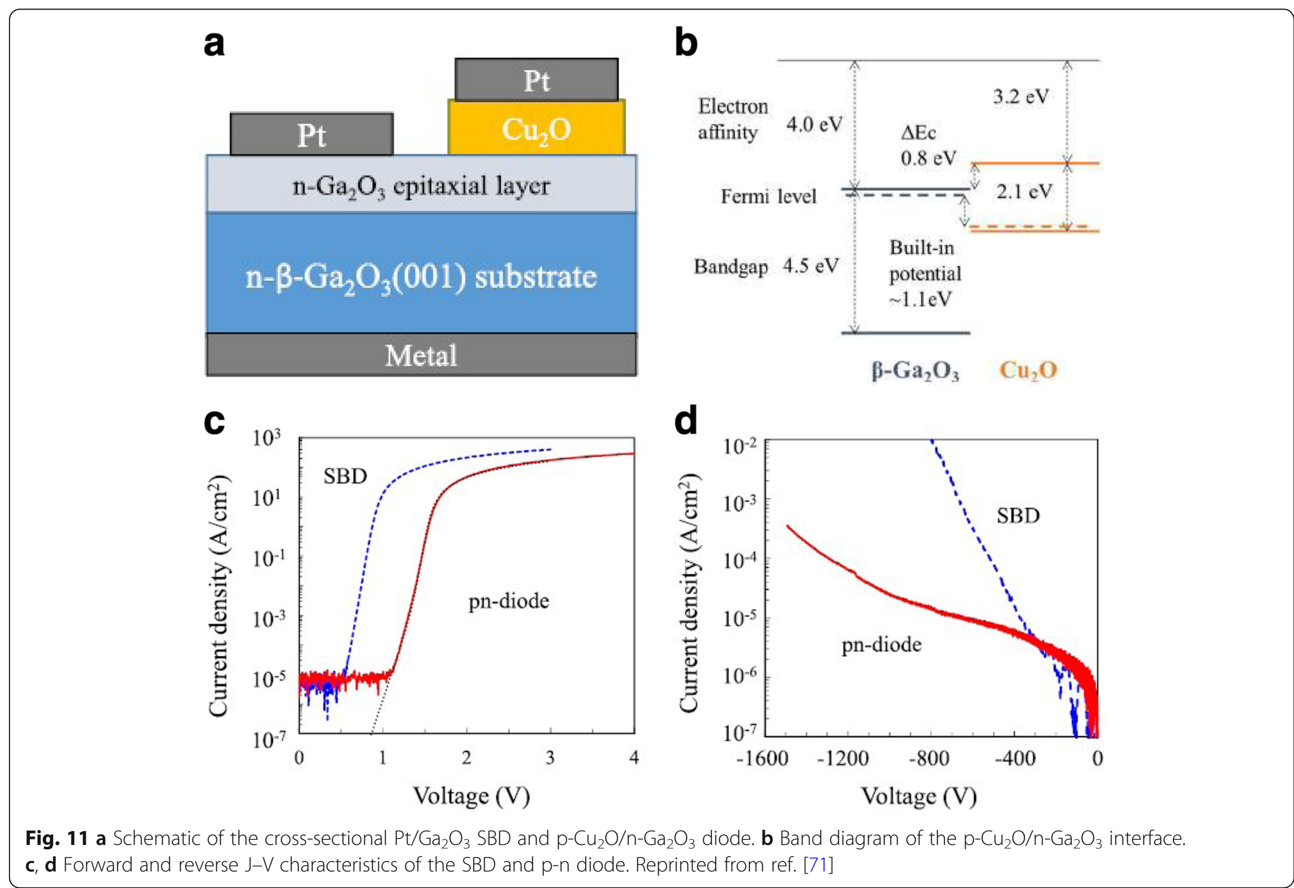

Fig. 11 a Schematic of the cross-sectional Pt/Ga_2O_3 SBD and p-Cu_2O/n-Ga_2O_3 diode. **b** Band diagram of the p-Cu_2O/n-Ga_2O_3 interface. **c**, **d** Forward and reverse J–V characteristics of the SBD and p-n diode. Reprinted from ref. [71]

reduced compared with the previous reports. This work is a valuable exploration on the advanced fabrication process of Ga_2O_3 SBD. In the 2nd International Workshop on Gallium Oxide and Related Materials (IWGO 2017) held in Italy, they further reported the improved trench SBD. The threshold voltage decreased to 0.5 V. On-resistance was 2.4 mΩ cm^2, and breakdown voltage was over 400 V. Compared to the commercialized 600 V SiC SBD, the improved trench Ga_2O_3 SBD exhibited superiority in switching loss.

To date, there has been no effective p-type doping in Ga_2O_3, so bipolar devices are not easy to be realized. In 2017, T. Watahiki et al. from Mitsubishi Electric Corporation reported a heterojunction p-Cu_2O/n-Ga_2O_3 p-n diode without local termination structure [71]. Figure 11 shows the schematic, band diagram and J–V curves of this p-n diode. Pt/Ga_2O_3 SBD was simultaneously fabricated and measured for comparison. The breakdown voltage of the p-n diode reached as high as 1.49 kV. The on-resistance was 8.2 mΩ cm^2, much lower than that of the SBD with a thick drift layer reported by J. Yang et al. [69]. So, it can be found that bipolar Ga_2O_3 device has a certain advantage over unipolar device in regard to the low on-resistance. This work provides a possible solution for the design Ga_2O_3-based bipolar devices. However, this p-n diode exhibited a high threshold voltage (1.7 V). Moreover, in bipolar device, there is the minority carrier storage effect. With the improvement of SBD device structure, this p-n diode appears to show significant competitivity in the aspect of 600–1200 V voltage-resistant level and high frequency. It is believed that with the continuous exploration on the materials, SBD might still be a more effective approach for development of the high-voltage Ga_2O_3 device before the successful preparation of p-type Ga_2O_3.

In practical applications, SBD is usually used to rectify the AC or pulse signals as a rectifier in a circuit. It should work at different frequencies. Q. He et al. from IMECAS investigated the rectification characteristics of the Pt/

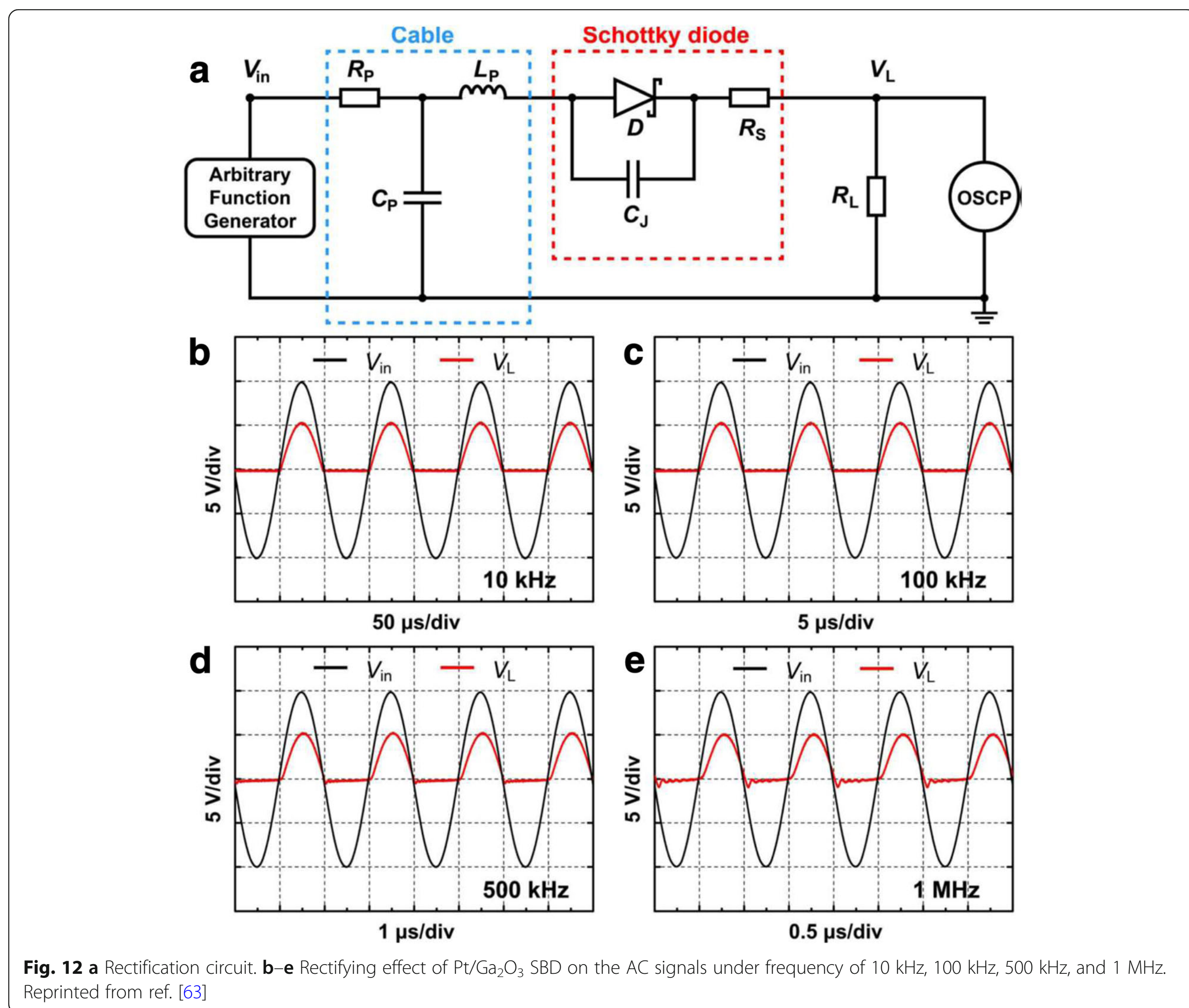

Fig. 12 a Rectification circuit. **b**–**e** Rectifying effect of Pt/Ga_2O_3 SBD on the AC signals under frequency of 10 kHz, 100 kHz, 500 kHz, and 1 MHz. Reprinted from ref. [63]

Ga_2O_3 SBD under the AC frequency under 10 kHz to 1 MHz by using a half-wave rectification circuit (Fig. 12) [63]. The testing result proves that the device has the ideal working frequency of 100 kHz, which is equivalent to that of SiC. This work is beneficial for people to further explore how Ga_2O_3 Schottky rectifier can operate at higher frequency and also to construct power circuit modules based on Ga_2O_3 SBD single device.

Table 2 lists and compares the basic performance parameters of some typical Ga_2O_3 Schottky barrier diode reported since 2012. From this table, it is apparent that with the improvement of device structure and fabrication processes, the performances are getting better and better.

Conclusions

Currently, Ga_2O_3 SBD is still in its early stage. With the continuous development of fabrication processes, device structure becomes more and more complicated. At the same time, the improvement of the quality of single-crystal substrates and epitaxial films also significantly push forward device performances. However, to date, the development process of Ga_2O_3 SBD is very similar to those of previous Si SBD and SiC SBD. Furthermore, the research works on the intrinsic properties of Ga_2O_3 materials are still very few. But it is believed that on the basis of its ultra-wide bandgap of 4.7–4.9 eV and the development of device structure, Ga_2O_3 will better display its unique application value, which requires the joint efforts of the researchers.

Table 2 Basic performance parameters of reported Ga_2O_3 Schottky barrier diode since 2012

Device structure	n	$N_d - N_a$ (cm^{-3})	$J_{@2V}$ (A/cm^2)	R_s ($m\Omega\cdot cm^2$)	R_{on} ($m\Omega\cdot cm^2$)	qV_{bi} (eV)	$q\Phi_b$ (eV)	J_s (A/cm^2)	V_{br} (V)	Structure	Reference
Pt/(100)β-Ga_2O_3/Ti	1.1	2×10^{17}	421	2.8	2.9	0.63	0.9	2×10^{-16}	~ 200	Wafer	Our work, 2018 IEEE EDL [63]
Pt/(010)β-Ga $_2O_3$/Ti	1.1	2.3×10^{14}	56	9	12.5	1.07	1.3–1.4	2×10^{-16}	> 40	Wafer	Our work, 2017 APL [60]
Ni/(100)β-$(AlGa)_2O_3$/Ti	2.3	4.5×10^{18} (sub)	7.7 (1.7 V)	30.1	63.6	–	0.81	–	–	Epi-layer	Xidian University, China 2018 APL [66]
Ni/(001)β-Ga_2O_3/Ti	1.03	3.6×10^{18} (sub)	–	–	80	–	1.07	–	97	Epi-layer	UF, USA 2018 IEEE Trans. Electron Devices [72]
Mo/(001)β-Ga_2O_3/Ti	–	5 6×10^{16} (5 μm) 6×10^{18} (570 μm)	~ 200 (1 V)	–	1.9–2.4	~ 0.5	–	–	> 400	TMBS	Novel Crystal Tecnology, Inc., Japan IWGO 2017
Ni/(−201)β-Ga_2O_3/Ti	1.07	4×10^{15} (10 μm) 3.6×10^{18} (650 μm)	–	–	1.6–25	–	1.22	–	~ 1600	Epi-layer	UF, USA 2017 EDL [69]
Cu/(001)β-Ga_2O_3/Ti	1.1	6×10^{16} (7 μm) 2.5×10^{18} (350 μm)	~ 210 (1.5 V)	–	2.9	0.7–0.8	1.07	–	230	TMBS	Novel Crystal Tecnology, Inc., Japan 2017 EDL [70]
Ni/(001)β-Ga_2O_3/Ti	1.08	2×10^{16} (10 μm) 3.6×10^{18} (650 μm)	–	–	6	–	1.1	–	1016	Epi-layer	UF, USA 2017 APL [73]
Pt/(001)β-Ga2O3/Ti	1.03 ± 0.02	1.8×10^{16}	~ 80	–	5.1	1.32	1.46	–	1076	Field plate	NICT, Japan 2017 APL [68]
Ni/(010)β-Ga_2O_3/Sn	1.21–3.38	UID (2 μm) 4.1×10^{18} (650 μm)	–	–	–	–	0.95–1.01	–	210	Epi-layer	Korea, 2017 SST [74]
Pt/α-Ga_2O_3/Ti	–	–	3000	–	0.1	1.5–1.6	–	–	531	Film	FLOSFIA, Inc., Japan 2016 APE [18]
	–	–	1350	–	0.4	1.5–1.6	–	–	855	Film	
Ni/(−201)β-Ga_2O_3/Ti	1.19	2.6×10^{16}	< 1	51.8	–	–	1.04–1.12	–	–	–	USA, 2016 SST [75]
Pt/(001)β-Ga_2O_3/Ti	1.03 ± 0.01	1×10^{16}	> 100	–	3	1.0–1.1	1.12 ± 0.03	–	500	Epi-layer	NICT, Japan 2016 APL [16]
Pt/(010)β-Ga_2O_3/Ti	1.04–1.06	3×10^{16}	~ 100	–	7.85	1.23	1.3–1.5	6.5×10^{-19}	150	Wafer	Japan, 2013 EDL [62]
	–	5×10^{16}	> 100	–	4.3	1.23	–	9×10^{-19}	120	Wafer	
Cu/(−201)β-Ga_2O_3/Ti	1.2–1.4	8×10^{17}	~ 10	–	–	1.44	0.88–0.95	–	–	Wafer	Germany, 2013 PSS [76]
Au/(100)β-Ga_2O_3	1.02–1.09	6×10^{16}– 8×10^{17}	< 1	–	–	–	1.07 ± 0.05	–	–	Wafer	Germany, 2012 APL [77]

Abbreviations

AC: Alternating current; BFOM: Baliga's figure of merit; CVD: Chemical vapor deposition; EFG: Edge-defined film-fed growth; FFT: Fast Fourier transform; FP: Field plat; FZ: Floating zone; HRTEM: High-resolution transmission electron microscopy; HVPE: Halide vapor-phase epitaxy; IMECAS: Institute of Microelectronics of Chinese Academy of Sciences; MOCVD: Metal-organic chemical vapor deposition; MOSFET: Metal-oxide-semiconductor field-effect transistor; NICT: National Institute of Information and Communications Technology; PLD: Pulsed laser deposition; SBD: Schottky barrier diode; TE: Thermionic emission; TFE: Thermionic field emission; WBG: Wide bandgap; XRD: X-ray diffraction

Funding

This work was supported by the National Key R@D Program of China under Grant No. 2018YFB0406504.

Availability of Data and Materials

The dataset is available without restriction.

Authors' Contributions

XHW determined the text framework and wrote the manuscript. HQM, JGZ, LSB, PT and LM helped to review and discuss the manuscript. All authors read and approved the final manuscript.

Competing Interests

The authors declare that they have no competing interests.

Publisher's Note

Springer Nature remains neutral with regard to jurisdictional claims in published maps and institutional affiliations.

Author details

[1]College of Mechanical and Electrical Engineering, Sichuan Agricultural University, Yaan 625014, China. [2]Key Laboratory of Microelectronic Devices & Integration Technology, Institute of Microelectronics of Chinese Academy of Sciences, Beijing 100029, China. [3]School of Microelectronics, University of Science and Technology of China, Hefei 230026, China.

Received: 3 August 2018 Accepted: 6 September 2018
Published online: 19 September 2018

References

1. Baliga BJ (2010) Fundamentals of power semiconductor devices. Springer Science & Business Media, New York
2. Millán J, Godignon P, Perpiñà X, Pérez-Tomás A, Rebollo J (2014) A survey of wide bandgap power semiconductor devices. IEEE Trans Power Electron 29(5):2155–2163
3. Fujita S (2015) Wide-bandgap semiconductor materials: for their full bloom. Jpn J Appl Phys 54(3):030101
4. Higashiwaki M, Sasaki K, Kuramata A, Masui T, Yamakoshi S (2014) Development of gallium oxide power devices. Phys Status Solidi 211(1):21–26
5. Higashiwaki M, Sasaki K, Murakami H, Kumagai Y, Koukitu A, Kuramata A, Masui T, Yamakoshi S (2016) Recent progress in Ga_2O_3 power devices. Semicond Sci Technol 31(3):034001
6. Tippins HH (1965) Optical absorption and photoconductivity in the band edge of β-Ga_2O_3. Phys Rev 140(1A):316–319
7. Orita M, Ohta H, Hirano M, Hosono H (2000) Deep-ultraviolet transparent conductive β-Ga_2O_3 thin films. Appl Phys Lett 77(25):4166–4168
8. He H, Orlando R, Blanco MA, Pandey R, Amzallag E, Baraille I, Rérat M (2006) First-principles study of the structural, electronic, and optical properties of Ga_2O_3 in its monoclinic and hexagonal phases. Phys Rev B 74(19):195123
9. Onuma T, Saito S, Sasaki K, Masui T, Yamaguchi T, Honda T, Higashiwaki M (2015) Valence band ordering in β-Ga_2O_3 studied by polarized transmittance and reflectance spectroscopy. Jpn J Appl Phys 54(11):112601
10. Sasaki K, Kuramata A, Masui T, Víllora EG, Shimamura K, Yamakoshi S (2012) Device-quality β-Ga_2O_3 epitaxial films fabricated by ozone molecular beam epitaxy. Appl Phys Express 5(5):5502
11. Pearton SJ, Yang J, Cary PH, Ren F, Kim J, Tadjer MJ, Mastro MA (2018) A review of Ga_2O_3 materials, processing, and devices. Appl Phys Rev 5(1):011301
12. Ueda N, Hosono H, Waseda R, Kawazoe H (1997) Synthesis and control of conductivity of ultraviolet transmitting β-Ga_2O_3 single crystals. Appl Phys Lett 70(26):3561–3563
13. Víllora EG, Shimamura K, Yoshikawa Y, Aoki K, Ichinose N (2004) Large-size β-Ga_2O_3 single crystals and wafers. J Cryst Growth 270(3–4):420–426
14. Aida H, Nishiguchi K, Takeda H, Aota N, Sunakawa K, Yaguchi Y (2008) Growth of β-Ga_2O_3 single crystals by the edge-defined, film fed growth method. Jpn J Appl Phys 47(11):8506–8509
15. Oishi T, Koga Y, Harada K, Kasu M (2015) High-mobility β-Ga_2O_3 (-201) single crystals grown by edge-defined film-fed growth method and their schottky barrier diodes with Ni contact. Appl Phys Express 8(3):031101
16. Higashiwaki M, Konishi K, Sasaki K, Goto K, Nomura K, Thieu QT, Togashi R, Murakami H, Kumagai Y, Bo M (2016) Temperature-dependent capacitance–voltage and current–voltage characteristics of Pt/Ga_2O_3 (001) schottky barrier diodes fabricated on n–Ga_2O_3 drift layers grown by halide vapor phase epitaxy. Appl Phys Lett 108(13):1759–1728
17. Kuramata A, Koshi K, Watanabe S, Yamaoka Y, Masui T, Yamakoshi S (2016) High-quality beta-Ga_2O_3 single crystals grown by edge-defined film-fed growth. Jpn J Appl Phys 55(12):1202A2
18. Oda M, Tokuda R, Kambara H, Tanikawa T, Sasaki T, Hitora T (2016) Schottky barrier diodes of corundum-structured gallium oxide showing on-resistance of 0.1 mΩ cm2 grown by mist epitaxy®. Appl Phys Express 9(2):021101
19. Choi JH, Cho CH, Cha HY (2018) Design consideration of high voltage Ga_2O_3 vertical schottky barrier diode with field plate. Results Phys 9:1170–1171
20. Fu H, Chen H, Huang X, Baranowski I, Montes J, Yang T-H, Zhao Y (2018) A comparative study on the electrical properties of vertical (201) and (010) beta-Ga_2O_3 schottky barrier diodes on EFG single-crystal substrates. IEEE Trans Electron Devices 65(8):3507–3513
21. Yang J, Ren F, Tadjer M, Pearton SJ, Kuramata A (2018) Ga_2O_3 schottky rectifiers with 1 ampere forward current, 650 V reverse breakdown and 26.5 MW. cm(−2) figure-of-merit. AIP Adv 8(5):055026
22. Hu Z, Zhou H, Dang K, Cai Y, Feng Z, Gao Y, Feng Q, Zhang J, Hao Y (2018) Lateral beta-Ga_2O_3 Schottky barrier diode on sapphire substrate with reverse blocking voltage of 1.7 KV. IEEE J Electron Devi 6(1):815–820
23. Joishi C, Rafique S, Xia Z, Han L, Krishnamoorthy S, Zhang Y, Lodha S, Zhao H, Rajan S (2018) Low-pressure CVD-grown beta-Ga_2O_3 bevel-field-plated schottky barrier diodes. Appl Phys Express 11(3):031101
24. Yang J, Ren F, Tadjer M, Pearton SJ, Kuramata A (2018) 2300V reverse breakdown voltage Ga_2O_3 schottky rectifiers. ECS J Solid State Sci Technol 7(5):Q92–Q96
25. Higashiwaki M, Sasaki K, Kamimura T, Hoi Wong M, Krishnamurthy D, Kuramata A, Masui T, Yamakoshi S (2013) Depletion-mode Ga_2O_3 metal-oxide-semiconductor field-effect transistors on beta-Ga_2O_3 (010) substrates and temperature dependence of their device characteristics. Appl Phys Lett 103(12):013504
26. Higashiwaki M, Sasaki K, Kuramata A, Masui T, Yamakoshi S (2012) Gallium oxide (Ga_2O_3) metal-semiconductor field-effect transistors on single-crystal β-Ga_2O_3 (010) substrates. Appl Phys Lett 100(1):013504
27. Hwang WS, Verma A, Peelaers H, Protasenko V (2014) High-voltage field effect transistors with wide-bandgap β-Ga_2O_3 nanomembranes. Appl Phys Lett 104(20):1229–1213
28. Kamimura T, Sasaki K, Man HW, Krishnamurthy D, Kuramata A, Masui T, Yamakoshi S, Higashiwaki M (2014) Band alignment and electrical properties of Al_2O_3/β-Ga_2O_3 heterojunctions. Appl Phys Lett 104(19):A316–A317
29. Jia Y, Zeng K, Wallace JS, Gardella JA, Singisetti U (2015) Spectroscopic and electrical calculation of band alignment between atomic layer deposited SiO_2 and β-Ga_2O_3 (−201). Appl Phys Lett 106(10):A316–A319
30. Roy R, Hill VG, Osborn EF (1952) Polymorphism of Ga_2O_3 and the system Ga_2O_3—H_2O. J Am Chem Soc 74(3):719–722
31. Higashiwaki M, Jessen G H (2018) Guest editorial: the dawn of gallium oxide microelectronics. Appl Phys Lett 112(6):060401.
32. Janotti A, Van DW, Chris G (2005) Oxygen vacancies in ZnO. Appl Phys Lett 87(12):125210
33. Oshima T, Kaminaga K, Mukai A, Sasaki K, Masui T, Kuramata A, Yamakoshi S, Fujita S, Ohtomo A (2013) Formation of semi-insulating layers on semiconducting β-Ga_2O_3 single crystals by thermal oxidation. Jpn J Appl Phys 52(5R):051101
34. Varley JB, Weber JR, Janotti A, Van de Walle CG (2010) Oxygen vacancies and donor impurities in β-Ga_2O_3. Appl Phys Lett 97(14):3561
35. Hajnal Z, Miro J, Kiss G, Reti F (1999) Role of oxygen vacancy defect states in the n-type conduction of β-Ga_2O_3. J Appl Phys 86(7):3792–3796
36. Fleischer M, Giber J, Meixner H (1992) H_2-induced changes in electrical conductance of β-Ga_2O_3 thin-film systems. Appl Phys A Mater Sci Process 54(6):560–566

37. Becker F, Krummel C, Freiling A, Fleischer M, Kohl C (1997) Decomposition of methane on polycrystalline thick films of Ga_2O_3 investigated by thermal desorption spectroscopy with a mass spectrometer. Fresenius J Anal Chem 358(1–2):187–189
38. Schwebel T, Fleischer M, Meixner H, Kohl CD (1998) Co-sensor for domestic use based on high temperature stable Ga_2O_3 thin films. Sens Actuators B Chem 49(1–2):46–51
39. Ogita M, Higo K, Nakanishi Y, Hatanaka Y (2001) Ga_2O_3 thin film for oxygen sensor at high temperature. Appl Surf Sci 175(01):721–725
40. Bae J, Kim HW, Kang IH, Yang G, Kim J (2018) High breakdown voltage quasi-two-dimensional β-Ga_2O_3 field-effect transistors with a boron nitride field plate. Appl Phys Lett 112(12):122102
41. Zhou H, Si M, Alghamdi S, Qiu G, Yang L, Ye P (2017) High performance depletion/enhancement-mode β-Ga_2O_3 on insulator (GOOI) field-effect transistors with record drain currents of 600/450 mA/mm. IEEE Electron Device Lett 38(1):103–106
42. Ahn S, Ren F, Kim J, Oh S, Kim J, Mastro MA, Pearton SJ (2016) Effect of front and back gates on β-Ga_2O_3 nano-belt field-effect transistors. Appl Phys Lett 109(6):192–1338
43. Zhou H, Maize K, Qiu G, Shakouri A, Ye PD (2017) β-Ga_2O_3 on insulator field-effect transistors with drain currents exceeding 1.5 A/mm and their self-heating effect. Appl Phys Lett 111(9):092102
44. Zhao B, Wang F, Chen H, Wang Y, Jiang M, Fang X, Zhao D (2015) Solar-blind avalanche photodetector based on single ZnO-Ga_2O_3 core-shell microwire. Nano Lett 15(6):3988
45. Chen H, Liu K, Hu L, Al-Ghamdi AA, Fang X (2015) New concept ultraviolet photodetectors. Mater Today 18(9):493–502
46. Sang L, Liao M, Sumiya M (2013) A comprehensive review of semiconductor ultraviolet photodetectors: from thin film to one-dimensional nanostructures. Sensors 13(8):10482–10518
47. Higashiwaki M, Kuramata A, Murakami H, Kumagai Y (2017) State-of-the-art technologies of gallium oxide (Ga_2O_3) power devices. J Phys D Appl Phys 50(33):333002
48. Teherani FH, Khodaparast GA, Xu YV, Wu J, Dravid VP, Pavlidis D, Razeghi M, Mcclintock R, Rogers DJ, Park JH (2018) A review of the growth, doping, and applications of beta-Ga_2O_3 thin films, Oxide-based Materials and Devices IX. International Society for Optics and Photonics. San Francisco. 10533:105330R. https://doi.org/10.1117/12.2302471
49. Sasaki K, Higashiwaki M, Kuramata A, Masui T, Yamakoshi S (2013) Si-ion implantation doping in β-Ga_2O_3 and its application to fabrication of low-resistance ohmic contacts. Appl Phys Express 6(4):086502
50. Mu W, Jia Z, Yin Y, Hu Q, Zhang J, Feng Q, Hao Y, Tao X (2017) One-step exfoliation of ultra-smooth β-Ga_2O_3 wafers from bulk crystal for photodetectors. CrystEngComm 19(34):5122–5127
51. Guo Z, Verma A, Wu X, Sun F, Hickman A, Masui T, Kuramata A, Higashiwaki M, Jena D, Luo T (2015) Anisotropic thermal conductivity in single crystal β-gallium oxide. Appl Phys Lett 106(11):591
52. Handwerg M, Mitdank R, Galazka Z, Fischer SF (2015) Temperature-dependent thermal conductivity in mg-doped and undoped β-Ga_2O_3 bulk-crystals. Semicond Sci Technol 30(2):24006–24010(24005)
53. Santia MD, Tandon N, Albrecht JD (2015) Lattice thermal conductivity in β-Ga_2O_3 from first principles. Appl Phys Lett 92(4):184
54. Ma N, Tanen N, Verma A, Guo Z, Luo T, Xing H, Jena D (2016) Intrinsic electron mobility limits in β-Ga_2O_3. Appl Phys Lett 109(21):A316
55. Higashiwaki M, Murakami H, Kumagai Y, Kuramata A (2016) Current status of Ga_2O_3 power devices. Jpn J Appl Phys 55(12):1202A1
56. Ahn S, Ren F, Yuan L, Pearton SJ, Kuramata A (2017) Temperature-dependent characteristics of Ni/Au and Pt/Au Schottky diodes on beta-Ga_2O_3. ECS J Solid State Sci Technol 6(1):P68–P72
57. Yao Y, Gangireddy R, Kim J, Das KK, Davis RF, Porter LM (2017) Electrical behavior of β-Ga_2O_3 Schottky diodes with different schottky metals. J Vac Sci Technol B Nanotechnol Microelectron 35(3):03D113
58. Farzana E, Zhang Z, Paul PK, Arehart AR, Ringel SA (2017) Influence of metal choice on (010) β-Ga_2O_3 Schottky diode properties. Appl Phys Lett 110(20):013504
59. Tadjer MJ, Wheeler VD, Shahin DI, Eddy CR Jr, Kub FJ (2017) Thermionic emission analysis of TiN and Pt Schottky contacts to beta-Ga_2O_3. ECS J Solid State Sci Technol 6(4):P165–P168
60. He Q, Mu W, Dong H, Long S, Jia Z, Lv H, Liu Q, Tang M, Tao X, Liu M (2017) Schottky barrier diode based on β-Ga_2O_3 (100) single crystal substrate and its temperature-dependent electrical characteristics. Appl Phys Lett 110(9):093503
61. Jian G, He Q, Mu W, Fu B, Dong H, Qin Y, Zhang Y, Xue H, Long S, Jia Z (2018) Characterization of the inhomogeneous barrier distribution in a Pt/(100) β-Ga_2O_3 schottky diode via its temperature-dependent electrical properties. AIP Adv 8(1):015316
62. Sasaki K, Higashiwaki M, Kuramata A, Masui T, Yamakoshi S (2013) Ga_2O_3 schottky barrier diodes fabricated by using single-crystal β-Ga_2O_3 (010) substrates. IEEE Electron Device Lett 34(4):493–495
63. He Q, Mu W, Fu B, Jia Z, Long S, Yu Z, Yao Z, Wang W, Dong H, Qin Y (2018) Schottky barrier rectifier based on (100) β-Ga_2O_3 and its DC and AC characteristics. IEEE Electron Device Lett 39(4):556–559
64. Feng Q, Hu Z, Feng Z, Xing X, Zuo Y, Yan G, Lu X, Zhang C, Zhou H, Zhang J (2018) Research on the growth of β-$(AlGa)_2O_3$ film and the analysis of electrical characteristics of Ni/Au Schottky contact using Tung's model. Superlattices Microstruct 120:441–447
65. Li A, Feng Q, Zhang J, Hu Z, Feng Z, Zhang K, Zhang C, Zhou H, Hao Y (2018) Investigation of temperature dependent electrical characteristics on Au/Ni/β-Ga_2O_3 Schottky diodes. Superlattices Microstruct 119:212–217
66. Feng Q, Feng Z, Hu Z, Xing X, Yan G, Zhang J, Xu Y, Lian X, Hao Y (2018) Temperature dependent electrical properties of pulse laser deposited Au/Ni/β-$(AlGa)_2O_3$ Schottky diode. Appl Phys Lett 112(7):072103
67. Kaneko K, Fujita S, Hitora T (2018) A power device material of corundum-structured α-Ga_2O_3 fabricated by mist epitaxy. Jpn J Appl Phys 57(2S2):02CB18
68. Konishi K, Goto K, Murakami H, Kumagai Y, Kuramata A, Yamakoshi S, Higashiwaki M (2017) 1-kv vertical Ga_2O_3 field-plated schottky barrier diodes. Appl Phys Lett 110(10):103506
69. Yang J, Ahn S, Ren F, Pearton SJ, Jang S, Kuramata A (2017) High breakdown voltage (−201) β-Ga_2O_3 schottky rectifiers. IEEE Electron Device Lett 38(7):906–909
70. Sasaki K, Wakimoto D, Thieu QT, Koishikawa Y, Kuramata A, Higashiwaki M, Yamakoshi S (2017) First demonstration of β-Ga_2O_3 trench MOS-type schottky barrier diodes. IEEE Electron Device Lett 38(6):783–785
71. Watahiki T, Yuda Y, Furukawa A, Yamamuka M, Takiguchi Y, Miyajima S (2017) Heterojunction p-Cu_2O/n-Ga_2O_3 diode with high breakdown voltage. Appl Phys Lett 111(22):222104
72. Yang J, Ren F, Pearton SJ, Kuramata (2018) A Vertical geometry, 2-A forward current Ga_2O_3 Schottky rectifiers on bulk Ga_2O_3 substrates. IEEE Trans Electron Devices 65(7):2790–2796
73. Yang J, Ahn S, Ren F, Pearton SJ, Jang S, Kim J, Kuramata A (2017) High reverse breakdown voltage Schottky rectifiers without edge termination on Ga_2O_3. Appl Phys Lett 110(19):030101
74. Oh S, Yang G, Kim J (2017) Electrical characteristics of vertical Ni/β-Ga_2O_3 schottky barrier diodes at high temperatures. ECS J Solid State Sci Technol 6(2):Q3022–Q3025
75. Jayawardena A, Ahyi AC, Dhar S (2016) Analysis of temperature dependent forward characteristics of Ni/(−201) Ga_2O_3 Schottky diodes. Semicond Sci Technol 31(11):115002
76. Splith D, Müller S, Schmidt F, von Wenckstern H, van Rensburg JJ, Meyer WE, Grundmann M (2014) Determination of the mean and the homogeneous barrier height of Cu Schottky contacts on heteroepitaxial β-Ga_2O_3 thin films grown by pulsed laser deposition. Phys Status Solidi A 211(1):40–47
77. Mohamed M, Irmscher K, Janowitz C, Galazka Z (2012) Schottky barrier height of Au on the transparent semiconducting oxide β-Ga_2O_3. Appl Phys Lett 101(13):132106
78. Müller S, von Wenckstern H, Schmidt F, Splith D, Heinhold R, Allen M, Grundmann M (2014) Method of choice for fabrication of high-quality ZnO-based Schottky diodes. J Appl Phys 116(19):194506
79. Yao Y, Davis RF, Porter LM (2017) Investigation of different metals as ohmic contacts to β-Ga_2O_3: comparison and analysis of electrical behavior, morphology, and other physical properties. J Electron Mater 46(4):2053–2060